

Allograft rejection is restrained by short-lived TIM-3⁺PD-1⁺Foxp3⁺ Tregs

Shipra Gupta,¹ Thomas B. Thornley,¹ Wenda Gao,¹ Rafael Larocca,¹ Laurence A. Turka,¹ Vijay K. Kuchroo,² and Terry B. Strom¹

¹Harvard Medical School, Department of Medicine, The Transplant Institute, Beth Israel Deaconess Medical Center, Boston, Massachusetts, USA. ²Center for Neurologic Diseases, Brigham and Women's Hospital, Boston, Massachusetts, USA.

Tregs play a pivotal role in inducing and maintaining donor-specific transplant tolerance. The T cell immunoglobulin and mucin domain-3 protein (TIM-3) is expressed on many fully activated effector T cells. Along with program death 1 (PD-1), TIM-3 is used as a marker for exhausted effector T cells, and interaction with its ligand, galectin-9, leads to selective death of TIM-3⁺ cells. We report herein the presence of a galectin-9-sensitive CD4⁺FoxP3⁺TIM-3⁺ population of T cells, which arose from CD4⁺FoxP3⁺TIM-3⁻ proliferating T cells in vitro and in vivo and were often PD-1⁺. These cells became very prominent among graft-infiltrating Tregs during allograft response. The frequency and number of TIM-3⁺ Tregs peaked at the time of graft rejection and declined thereafter. Moreover, these cells also arise in a tolerance-promoting donor-specific transfusion model, representing a pool of proliferating, donor-specific Tregs. Compared with TIM-3⁻ Tregs, TIM-3⁺ Tregs, which are often PD-1⁺ as well, exhibited higher in vitro effector function and more robust expression of CD25, CD39, CD73, CTLA-4, IL-10, and TGF- β but not galectin-9. However, these TIM-3⁺ Tregs did not flourish when passively transferred to newly transplanted hosts. These data suggest that a heretofore unrecognized graft-infiltrating, short-lived subset of Tregs can restrain rejection.

Introduction

A hallmark of an adaptive immune response is differentiation and clonal expansion of T effector cell (Teff) populations, including Th1, Th2, Th17 cells, and Tregs (1–4). T cell immunoglobulin and mucin domain protein (TIM) family proteins are type I membrane glycoproteins containing common structural motifs, namely an Ig V domain, a highly glycosylated mucin domain, and a cytoplasmic domain (5–7). TIM proteins are critical regulators of the balance between various effector and Tregs subsets (6, 8). TIM-3, first identified as a cell surface molecule expressed by fully differentiated Th1 cells (9), is also expressed by some Th17 cells (10) and by mouse CD11c⁺ DCs (11). The role of TIM-3 has been studied in Th1- and Th17-driven immune responses (7, 9, 10, 12). Galectin-9, expressed by a variety of cells including Tregs, is a ligand for TIM-3 (13). The stereospecific interaction of TIM-3 expressed upon fully differentiated Th1 cells with galectin-9, a molecule expressed by Tregs, triggers the selective death of TIM-3⁺ Th1 cells (13). In mice, the use of *Tim3*^{-/-} recipients or blockade of the interaction of TIM-3 with its ligands by TIM-3-Ig in wild-type recipients prevents the acquisition of dominant-type tolerance to MHC-mismatched allografts or nominal antigen (7, 14). TIM-3 and program death 1 (PD-1), another death molecule (15–17), are expressed by exhausted, dysfunctional Teffs, a population unable to proliferate or produce cytokines vigorously (18, 19). Overall, these studies implicate an important role for TIM-3 and PD-1 in governing the homeostasis of Th1/Th17 adaptive immune responses through the termination of the function and survival of these cytopathic T cells.

Tregs play a pivotal role in creation of donor-specific transplant tolerance (3, 20, 21). The TIM-3 to TIM-3 ligand interaction, almost certainly using galectin-9 as the TIM-3 ligand, is crucial for the induction of transplant tolerance (6, 7). In this study, we identify and characterize a subset of CD4⁺FoxP3⁺TIM-3⁺PD-1⁺ Tregs, which increase in frequency and heavily infiltrate the transplant as the allograft response proceeds. We hypothesized, albeit incorrectly, that the TIM-3⁺ Tregs, which are often PD-1⁺ as well, would be functionally impaired with respect to expression of Treg effector molecules and proliferation, as are TIM-3⁺ Th1 cells. To the contrary, we found that these cells possessed potent regulatory capacity in vitro but proved fragile when passively transferred into newly transplanted hosts. The characterization, origins, and role in immune system homeostasis of this Treg subset are explored.

Results

The number and frequency of CD4⁺FoxP3⁺TIM-3⁺ T cells, which are often PD-1⁺ as well, present during the allograft response peaks at the time of allograft rejection. CD4⁺TIM-3⁺Foxp3⁺ cells constitute about 2% to 5% of the total CD4⁺FoxP3⁺ population in the LNs and spleens of normal, nontransplanted C57BL/6 Foxp3GFP-KI (FoxP3 indicator) mice. The number and frequency of CD4⁺TIM-3⁺Foxp3⁺ cells increases with time after transplantation in the draining LNs (dLNs) and spleens of C57BL/6-KI recipients of BALB/c skin allografts as compared with that in recipients of syngeneic grafts. The number of CD4⁺TIM-3⁺Foxp3⁺ cells in dLNs and spleens, of which approximately two-thirds coexpress PD-1 (described below), peaked at day 7 after transplantation, the time of rejection, and fell to basal levels by day 11 after transplantation (Figure 1, A and B). At this time, CD4⁺Foxp3⁺TIM-3⁺ cells constituted 10%–15% of the CD4⁺FoxP3⁺ cells in dLN but were present in lesser abundance in nondraining LN and spleen (Supplemental Figure 1; supplemental material available online with this article; doi:10.1172/JCI45138DS1). About 40% of graft-infiltrating

Authorship note: Shipra Gupta and Thomas B. Thornley contributed equally to this work.

Conflict of interest: The authors have declared that no conflict of interest exists.

Citation for this article: *J Clin Invest.* 2012;122(7):2395–2404. doi:10.1172/JCI45138.

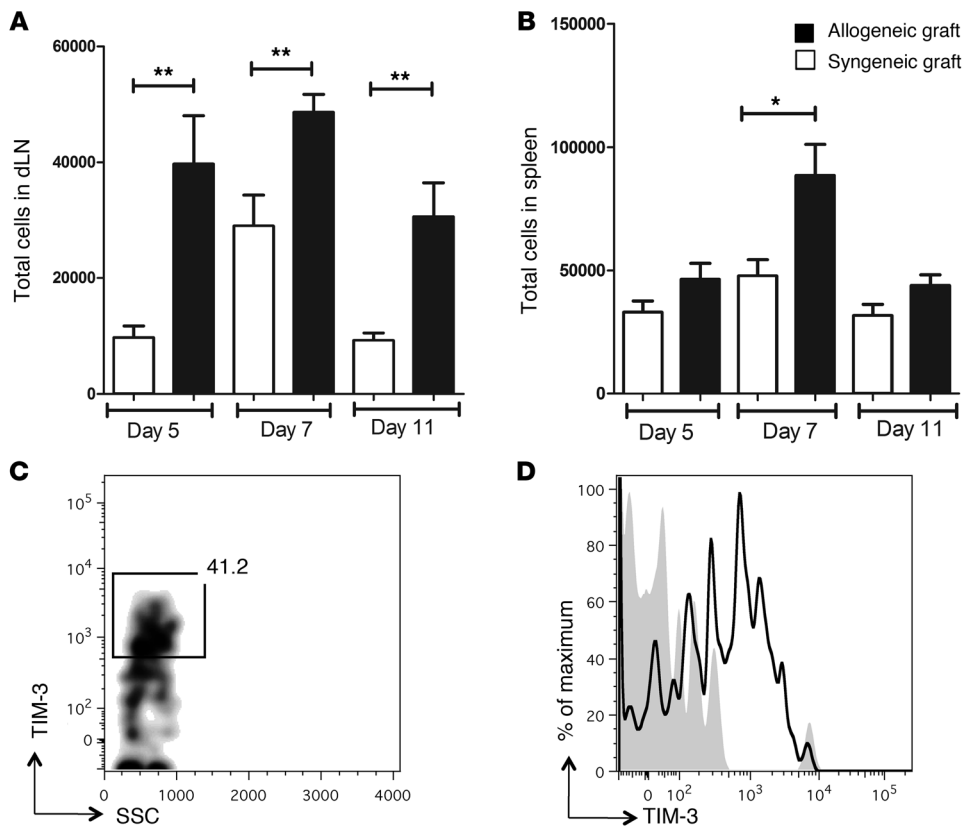


Figure 1

The number of CD4⁺FoxP3⁺TIM-3⁺ T cells within dLNs and spleens arising during the allograft response peak at graft rejection. Fully allogeneic BALB/c (H-2d) or syngeneic C57BL/6 (H-2b) full-thickness body skin was grafted on the lateral thorax of FoxP3 GFP-KI reporter C57BL/6 (H-2b) mice. C57BL/6-KI mice reject the BALB/c skin graft on day 7. The number of FoxP3-GFP⁺TIM-3⁺ cells in (A) dLNs and (B) spleens from skin transplant recipients was determined by flow cytometry ($n \geq 8$ mice). (A and B) The TIM-3⁺FoxP3⁺ T cells within dLNs and spleens peaked at the time of rejection and were more numerous in allogeneic as compared with syngeneic grafted hosts. Data are presented as mean \pm SEM; * $P < 0.05$; ** $P < 0.01$. (C) Gated CD4⁺GFP⁺FoxP3⁺ cells harvested from collagenase digested allogeneic skin transplants were analyzed for TIM-3 expression by flow cytometry. CD4⁺GFP⁺FoxP3⁺TIM-3⁺ Tregs comprised 40% of the graft-infiltrating Tregs on day 5 after transplantation. (D) The magnitude of TIM-3 expression on the TIM-3⁺ Tregs is depicted in comparison to the staining control. Gray shading represents fluorescence minus 1 for TIM-3 staining, and the black line represents TIM-3 expression on CD4⁺GFP⁺FoxP3⁺ cells in the graft ($n = 4$).

FoxP3⁺ cells were TIM-3⁺ at day 5 after transplantation (Figure 1C). Of these graft-infiltrating TIM-3⁺ Tregs, approximately half were PD-1⁺ (data not shown).

In the response to donor-specific transfusion CD4⁺FoxP3⁺TIM-3⁺ cells are donor specific. As the number and frequency of CD4⁺FoxP3⁺TIM-3⁺ cells peaked at time of rejection and then fell to basal levels, we hypothesized that many CD4⁺FoxP3⁺TIM-3⁺ cells may be donor reactive. We tested this hypothesis in a tolerance-promoting donor-specific transfusion (DST) model. In this model, DBA/2 splenocytes (H-2d, Mlsa) are transfused into BALB/c mice (H-2d, Mlsb), thereby stimulating expansion of donor-reactive Mlsa-specific V β 6⁺, but not Mlsa unresponsive V β 8⁺, CD4⁺ T cells (22, 23). Five days after DST, we analyzed spleens of DST-treated and control mice and noted a significant increase ($P < 0.0001$) in the percentage of CD4⁺TIM-3⁺Foxp3⁺ cells in the spleens of mice infused with DBA/2 DST (Figure 2A). Notably, this increase was associated with a 2.5-

fold increase in V β 6⁺Foxp3⁺TIM-3⁺, but not V β 8⁺Foxp3⁺TIM-3⁺, cells (Figure 2B), suggesting that the increase in the percentage of CD4⁺Foxp3⁺TIM-3⁺ cells, results, at least in part, from preferential expansion of a pool of donor-reactive Foxp3⁺ Tregs. A comparable increase in V β 6⁺ but not V β 8⁺ cells was also observed within the CD4⁺Foxp3⁺TIM-3⁻ compartment (data not shown).

CD4⁺TIM-3⁺ Tregs arise from a proliferating pool of CD4⁺TIM-3⁻ Tregs. The CD4⁺GFP⁺Foxp3⁺ cells obtained by cell sorting from non-transplanted C57BL/6-KI mice were cultured for 4 days with anti-CD3 and anti-CD28 in the presence or absence of IL-2. After 4 days, the TIM-3⁺ subset increased by 4- to 8-fold in the absence or presence of IL-2, respectively (MFI values: -IL-2, 2,020 arbitrary units; +IL-2, 1,970 arbitrary units) (Figure 3A). We next probed whether CD4⁺FoxP3⁺TIM-3⁺ cells arise from a CD4⁺FoxP3⁺TIM-3⁻ subset upon activation and/or whether a preexisting TIM-3⁺ fraction of Tregs proliferate in the presence of IL-2. The TIM-3⁻ Tregs were sorted from spleens of normal C57BL/6 mice and cultured as above in the presence or absence of anti-CD3, anti-CD28, and IL-2. Cultivation of TIM-3⁻ Tregs with anti-CD3 and anti-CD28 induced expression of TIM-3 on approximately 13% of TIM-3⁻FoxP3⁺ cells (Figure 3B). In the absence of anti-CD3, TIM-3 expression was not induced (Figure 3B). While IL-2 enhances

acquisition of the TIM-3⁺ phenotype by TIM-3⁻ Tregs cultured with anti-CD3 and anti-CD28, in the absence of anti-CD3, IL-2 does not induce expression of TIM-3.

We next determined whether CD4⁺FoxP3⁺TIM-3⁺ Tregs arise in vivo from CD4⁺FoxP3⁺TIM-3⁻ Tregs. CD4⁺GFP⁺(FoxP3⁺)TIM-3⁻ Tregs, for which GFP is an indicator for FoxP3, (~97% pure) were sorted from BALB/c-KI mice 5 days after DBA/2 DST infusion and injected into BALB/c *Rag2*^{-/-} recipients grafted with DBA/2 skin. Three weeks after injection, 30% of GFP⁺ Tregs in spleens expressed TIM-3 (Figure 3C). Interestingly, a similar proportion of TIM-3-expressing GFP⁺ Tregs was also observed in ungrafted BALB/c *Rag2*^{-/-} mice (Figure 3D), indicating that expansion during homeostatic proliferation drives TIM-3 expression upon activation on a subpopulation of Tregs. Thus, TIM-3 expression is induced upon CD4⁺FoxP3⁺TIM-3⁻ Tregs as a consequence of various stimuli that provoke proliferation of this subset.

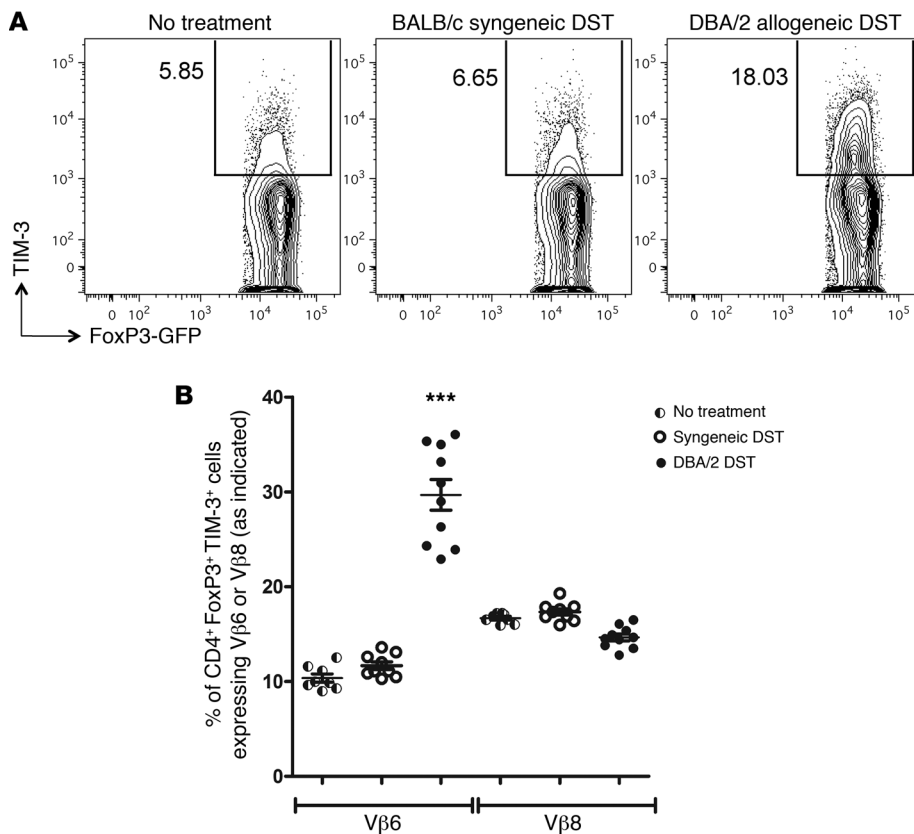


Figure 2 CD4⁺FoxP3⁺TIM-3⁺ cells are donor antigen specific. Five days after transfer of DBA/2 or BALB/c spleen cells into BALB/c-KI recipients, spleens were harvested and analyzed by flow cytometry in a tolerance-promoting DST model. Normal BALB/c-KI mice were used as controls. **(A)** CD4⁺GFP⁺FoxP3⁺ Tregs harvested from DST-treated or normal BALB/c-KI mice were stained for TIM-3 expression and **(B)** were further analyzed for donor-reactive Mlsa-specific Vβ6⁺ or donor unresponsive Vβ8⁺ CD4⁺ T cells. Numbers represent the percentage of CD4⁺GFP⁺FoxP3⁺ Tregs that are TIM-3⁺. Data are representative or mean ± SEM (*n* ≥ 8 animals); ****P* < 0.001.

CD4⁺Foxp3⁺TIM-3⁺ cells are often PD-1⁺ and bind annexin V but are neither dead nor exhausted at the time of graft rejection. TIM-3 expression by Tregs is a marker of senescent (13) or exhausted Tregs (18). As TIM-3⁺ Tregs stain positive for cell surface phosphatidylserine (annexin V⁺) and fail to exclude vital dyes (13), we hypothesized that Foxp3⁺TIM-3⁺ cells would manifest signs of exhaustion and ongoing apoptosis. To test our hypothesis, skin-grafted mice were injected with BrdU i.p. 24 and 16 hours prior to cell harvesting. Surprisingly, 2.5 times more proliferating cells were found within the Foxp3⁺TIM-3⁺ subset as compared with Foxp3⁺TIM-3⁻ subset in the dLNs (Figure 4A) and spleens (data not shown). The PD-1 programmed death marker is upregulated on activated Tregs (24), and coexpression of PD-1 with TIM-3 on Tregs has been linked to T cell exhaustion (25). Over 70% of Foxp3⁺TIM-3⁺ cells, while only 30% of Foxp3⁺TIM-3⁻ cells, in the dLNs of these mice expressed PD-1 (Figure 4B). To further test our hypothesis, we analyzed CD4⁺Foxp3⁺TIM-3⁺ cells from dLNs and spleens of C57BL/6-KI recipients of BALB/c allogeneic skin on day 7 after transplantation by staining with annexin V, a probe that binds surface phosphatidylserine, and with a viability dye. As compared with the TIM-3⁻Foxp3⁺ subset, 50% more CD4⁺Foxp3⁺TIM-3⁺ cells were stained by annexin V (Figure 4C). We consistently observed a trend toward a higher percentage of annexin V⁺ Tregs in the TIM-3⁺ population, a population that also expressed PD-1 (Supplemental Figure 2). More interestingly, in comparison with TIM-3⁻PD-1⁻ Tregs, the TIM-3⁺PD-1⁺ Tregs showed a clear increase (*P* = 0.0008) in the intensity of annexin V staining, as demonstrated by MFI values (Supplemental Figure 2), indicating that Tregs coexpressing TIM-3 and PD-1

are more likely to perish. However, CD4⁺Foxp3⁺TIM-3⁺annexin V⁺ cells excluded LIVE/DEAD blue, a dye that identifies dead cells. In contrast, 85% of CD4⁺Foxp3⁺TIM-3⁺ Tregs were stained by annexin V, of which one-third to one-half of these cells were dead, as deduced by staining with the cell viability dye (Figure 4C). Contrary to our hypothesis, the Foxp3⁺TIM-3⁺PD-1⁺ or Foxp3⁺TIM-3⁻PD-1⁻ cells, subsets that arise during the allograft response, proliferated vigorously and were not exhausted or functionally impaired as Tregs.

Testing the hypothesis that CD4⁺Foxp3⁺TIM-3⁺ cells are vulnerable to galectin-9-induced death signals. Galectin-9 is a TIM-3 ligand that triggers apoptotic death of TIM-3⁺ Tregs over a period of 2 to 4 hours in vitro (13). As CD4⁺Foxp3⁺TIM-3⁺ cells obtained from spleens excluded vital dyes (Figure 4C), we tested whether these cells die after interaction with galectin-9 ex vivo. GFP⁺Foxp3⁺ cells were sorted from spleens of C57BL/6-KI recipients of allogeneic skin grafts on day 7 and cultured with 0.5 μM galectin-9/PBS for 4 hours. By 4 hours after treatment, 41.5% of CD4⁺Foxp3⁺TIM-3⁺ cells were dead while 13.4% of Foxp3⁺TIM-3⁻ cells died in the presence of galectin-9. (Figure 4D). Seventy-five percent of CD4⁺Foxp3⁺TIM-3⁺ cells obtained from spleens of grafted mice on the day of rejection were annexin V⁺ (Figure 4C). This population is fragile, because after sorting for GFP⁺Foxp3⁺ cells only 12% CD4⁺Foxp3⁺TIM-3⁺ cells stained as annexin V⁺ (Figure 4D, *t* = 0). During sorting, about 70% of CD4⁺Foxp3⁺TIM-3⁺ cells were lost, indicating that the lost cells were composed of the early apoptotic population of annexin V⁺TIM-3⁺ cells. Although Foxp3⁺TIM-3⁺ cells were not dead or exhausted at time of rejection, they were sensitive to galectin-9 and thus may be short lived.

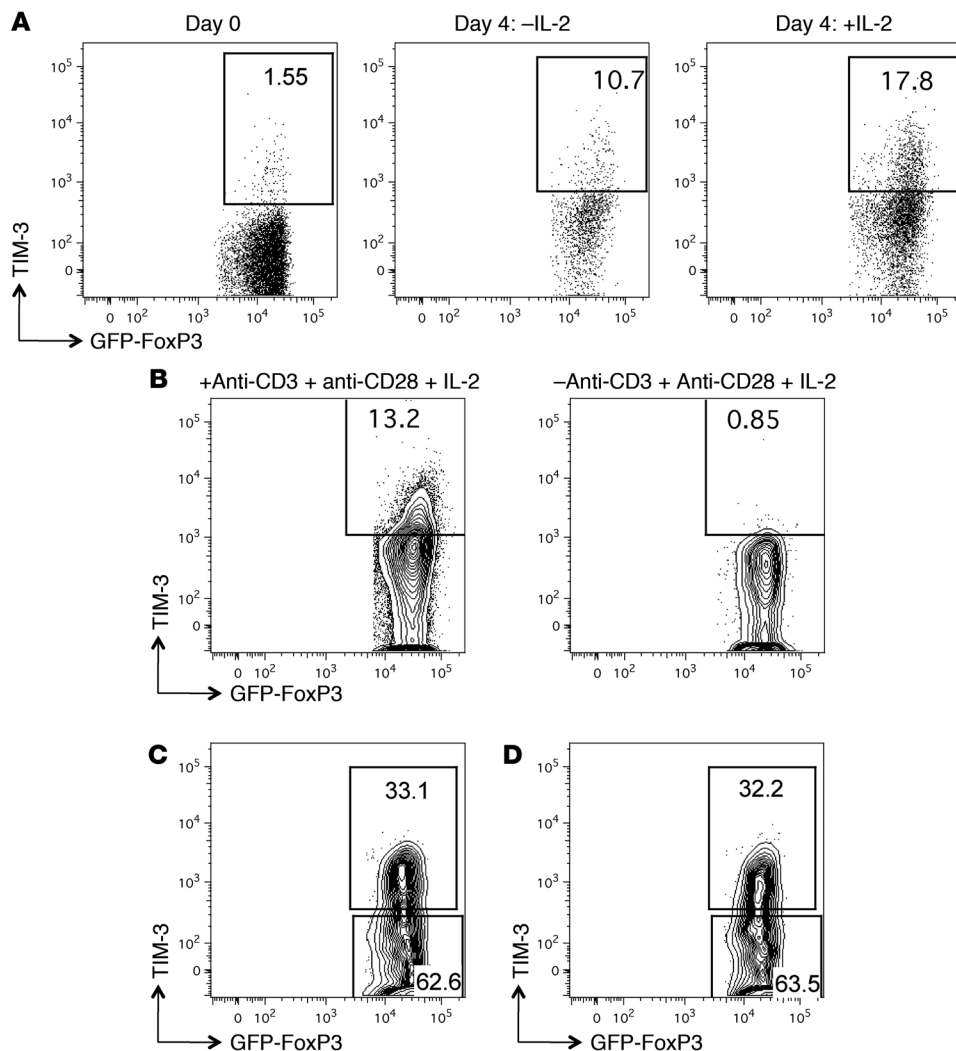


Figure 3

TIM-3 expression is induced in Tregs in vitro and in vivo on activation. CD4⁺GFP⁺FoxP3⁺ cells (total Tregs) sorted from spleens of unmanipulated mice were cultured in vitro in the presence of anti-CD3 (plate coated) and soluble anti-CD28 with or without IL-2. (A) Cells were analyzed for TIM-3 expression by flow cytometry on day 4. (B) TIM-3 expression is not induced in TIM-3⁻GFP⁺FoxP3⁺ cells (TIM-3⁻ Tregs) obtained from spleens of unmanipulated mice when cultured in vitro in the absence of anti-CD3, as indicated by flow cytometric analysis on day 4 (n = 3). Sorted GFP⁺(FoxP3⁺) TIM-3⁻ cells (TIM-3⁻ Tregs) from spleens of DBA/2 DST-infused BALB/c-KI mice were injected i.v. into (C) DBA/2 skin graft recipient BALB/c-Rag2^{-/-} mice or (D) ungrafted BALB/c-Rag2^{-/-} mice. Three weeks after transfer, CD4⁺GFP⁺(FoxP3⁺) spleen cells were analyzed for TIM-3 expression (n = 6). Numbers represent the percentage of CD4⁺GFP⁺FoxP3⁺ Tregs that are TIM-3⁺.

FoxP3⁺TIM-3⁺ Tregs are better suppressors in vitro than TIM-3⁻ Tregs and robustly express several Treg effector molecules. We compared the suppressive capacity of FoxP3⁺TIM-3⁺ regulatory cells and TIM-3⁻ Tregs in an in vitro mixed lymphocyte reaction (MLR). BALB/c-KI-TIM-3⁺/TIM-3⁻ Tregs were obtained from spleens by cell sorting 5 days after DBA/2 DST. Interestingly, TIM-3⁺ Tregs were more potent suppressors than the TIM-3⁻ Tregs at all Teff/Treg ratios studied (*P* < 0.01; Figure 5A). As Foxp3⁺TIM-3⁺ cells demonstrate more potent in vitro Treg effector function than their TIM-3⁻ counterparts, we hypothesized that these cells robustly express Treg effector molecules. Hence, we analyzed mRNA and cell surface level expression of various Treg effector molecules of Foxp3⁺TIM-3⁺ and Foxp3⁺TIM-3⁻ cells from dLNs of C57BL/6-KI recipients of allogeneic skin grafts on day 7. RNA was isolated from Foxp3⁺TIM-3⁺ and Foxp3⁺TIM-3⁻ cells obtained from dLNs of 30 to 35 pooled C57BL/6-KI-grafted mice. The gene and protein expression of CTLA-4, a vital Treg effector molecule whose expression is directly controlled by FoxP3 (26), was more robustly expressed by TIM-3⁺Foxp3⁺ cells than Foxp3⁺TIM-3⁻ cells in the dLNs (Figure 5, B and C). Moreover, 54.5% of CD4⁺Foxp3⁺TIM-3⁺ cells expressed CTLA-4 in contrast to only 20.8% of CD4⁺Foxp3⁺TIM-3⁻ cells (Figure 5C). The CD39 and CD73 ectonucleotidases are coexpressed

upon Tregs but not on Teffs and mediate adenosine-dependent immune suppression by Tregs (27). Interestingly, approximately 98% of CD4⁺Foxp3⁺TIM-3⁺ cells expressed CD39, in contrast to approximately 76% of CD4⁺Foxp3⁺TIM-3⁻ cells. A marked increase (2- to 2.5-fold) in the cell surface expression of CD39, but not of CD73, was observed among Foxp3⁺TIM-3⁺ cells in comparison to the that in the Foxp3⁺TIM-3⁻ subset (Figure 5, B and C). IL-10 and TGF-β are key mediators of suppression by Tregs in vivo (4, 28, 29). In comparison to Foxp3⁺TIM-3⁻ cells, Foxp3⁺TIM-3⁺ cells more robustly expressed IL-10 transcripts, and only an approximately 1.5 times increase in TGF-β transcripts was observed (Figure 5B). In comparison to CD4⁺Foxp3⁺TIM-3⁻ cells, 3 times more IL-10 protein expressing Tregs were present within the CD4⁺Foxp3⁺TIM-3⁺ cell compartment (Figure 5C). Galectin-9, moderately expressed on activated Tregs, binds to TIM-3 and aids termination of Teff responses by inducing death of TIM-3⁺ Th1/Th17 cells (13, 14). In contrast to other tested Treg effector molecules, galectin-9 was markedly reduced in the Foxp3⁺TIM-3⁺ cells as compared with that in the Foxp3⁺TIM-3⁻ cells (Figure 5B). IL-2 interaction with the trimolecular IL-2R complex, a complex that includes CD25, plays a key role in proliferation and maintenance of Tregs in the periphery (20, 30). Tregs express high copy num-



bers of CD25 transcripts and cell surface protein (30). Analysis of CD25 surface expression revealed, $\geq 95\%$ of Foxp3⁺TIM-3⁺ cells expressed CD25, and the cell surface copy number was 2.5 times that of Foxp3⁺TIM-3⁻ cells (Figure 5C). Hence, in comparison with Foxp3⁺TIM-3⁻ cells, a greater proportion of TIM-3⁺Foxp3⁺ cells not only expressed surface and soluble Treg functional markers in greater abundance but also CD25. Of the tested Treg markers, only galectin-9, the TIM-3 ligand, was downregulated on this subset of Tregs (Figure 5B). This situation may result from galectin-9-mediated death of TIM-3⁺ Tregs after contact with galectin-9⁺ Tregs. Galectin-9^{hi}TIM-3^{hi} Tregs may be subjected to elimination.

In vivo graft survival is less profoundly prolonged by adoptively transferred TIM-3⁺ Tregs than TIM-3⁻ Tregs. TIM-3⁺ Tregs expressed Treg effector molecules more robustly than TIM-3⁻ Tregs and thus are more potent suppressors in a 4-day in vitro MLR system (Figure 5). We further compared the suppressive ability of the Treg subsets in vivo. TIM-3⁺/TIM-3⁻ Tregs were sorted from spleens of DBA/2 DST-injected BALB/c-KI mice, by a process that was similar to the in vitro MLR. Teffs with or without TIM-3⁺/TIM-3⁻ Tregs (Teff/Treg = 2:1) were adoptively transferred into DBA/2 grafted BALB/c-Rag2^{-/-} mice, and graft survival was recorded. Injected TIM-3⁺ Tregs and Teffs prolonged graft survival (median survival time [MST], 19 d, $n = 6$) in comparison with the Teff-alone group (MST, 13 d, $n = 7$; Figure 6). However, DBA/2 skin grafts on mice injected with TIM-3⁻ Tregs and Teffs survived (MST, >120 d, $n = 6$) far longer than those on the mice injected with TIM-3⁺ Tregs and Teffs (Figure 6). Thus, and superficially paradoxical to the short term (72 hours) in vitro data, TIM-3⁺ Tregs were less potent suppressors in a more prolonged, several weeks long in vivo suppression assay than TIM-3⁻ Tregs. In BALB/c-KI mice injected with DBA/2 DST, the frequency of annexin V⁺ cells was 3-fold higher within the TIM-3⁺ Treg subset as compared with that within the TIM-3⁻ Treg subset after 5 days (Supplemental Figure 3). A clear increase in the intensity of annexin V staining was also observed for TIM-3⁺ Tregs as compared with that for TIM-3⁻ Tregs. To be effective in the in vivo assay, annexin V staining TIM-3⁺PD-1⁺ cells, bearing 2 death molecules, are likely to be already programmed for death, and Tregs must survive for a far longer period than they do in the MLR. It seems likely that many TIM-3⁺ Tregs, which are usually PD-1⁺ as well, perish during the prolonged in vivo assay test period. Hence, TIM-3⁺PD-1⁺ Tregs are paradoxically potent yet fragile. As the frequency of TIM-3⁺ Tregs is small, we could not compare potency of TIM-3⁺PD-1⁺ with TIM-3⁺PD-1⁻ Tregs in an in vivo transfer system.

Discussion

TIM-3, initially described as a Th1-specific marker belonging to the TIM family of proteins, fosters the specific elimination of TIM-3⁺ Teffs, e.g., Th1 and Th17, on interaction with its ligand galectin-9 (7, 13, 14, 18). Often coexpressed with TIM-3, PD-1 is also a marker expressed upon underperforming dysfunctional CD4⁺ and CD8⁺ T cells (18, 19). Based on these studies, we hypothesized that TIM-3 expression on Tregs would identify a senescent or exhausted subpopulation of Tregs.

In a fully allogeneic mouse skin transplant model, we have identified a subset of graft-infiltrating Tregs that expresses TIM-3 (ca. 40% of all graft-infiltrating Tregs as rejection becomes apparent), of which, about half coexpress PD-1 (data not shown). The number and frequency of CD4⁺FoxP3⁺TIM-3⁺ cells increased in recipient lymphoid tissues, peaked at the time of rejection, and fell to basal levels thereafter, likely due to a combination of cell death and the clearance of antigen that drives proliferation. The physiological proinflam-

matory and proliferative cytokine milieu during surgical intervention and healing process may contribute to the observed increase in TIM-3⁺ Tregs in dLNs of syngeneic graft recipients on day 7, which is significantly lower than that for allogeneic graft recipients. Indeed, TIM-3⁺ Tregs comprise a major proportion of skin graft-infiltrating Tregs. The TIM-3⁺ Treg subset is enriched for donor reactivity as (a) after DST, expansion of a donor-directed CD4⁺FoxP3⁺TIM-3⁺ V β 6-TCR, but not V β 8-TCR, Treg subset was observed in a tolerance-promoting model, wherein DBA/2 splenocytes (H-2d, Mlsa) transfused into BALB/c mice (H-2d, Mlsb) stimulated expansion of donor-reactive Mlsa-specific V β 6⁺, but not Mlsa unresponsive V β 8⁺, CD4⁺ T cells; (b) CD4⁺FoxP3⁺TIM-3⁺ T cells were particularly prominent, ca. 40% of graft-infiltrating Tregs, as clinically apparent rejection begins; (c) during the allograft response, TIM-3⁺ Tregs proliferated more vigorously than TIM-3⁻ Tregs; and (d) contraction of the TIM-3⁺PD-1⁺ Tregs after transplantation was more profound than contraction of TIM-3⁻ Tregs after graft rejection.

Both in vitro and in vivo studies demonstrated that TIM-3⁺ Tregs emerge from the TIM-3⁻ Treg subset. Anti-CD3/CD28-mediated activation in vitro of Tregs stimulates emergence of a TIM-3⁺ Treg population. TIM-3⁺ Tregs also arise from CD4⁺FoxP3⁺TIM-3⁻ cells in vivo during homeostatic proliferation. Hence, physiological processes leading to Treg expansion in the allograft response drive expression of TIM-3 by Tregs.

An intracellular PD-1 protein pool is detected in resting Tregs, whereas cell surface expression of PD-1 is detected on activated Tregs (24). Here, we have noted that 75% to 80% of TIM-3⁺ Tregs express cell surface PD-1 molecules in the dLNs of mice challenged with a skin allograft. Expression of inhibitory receptor PD-1 on Teffs is associated with imminent cell death. Tregs that coexpress TIM-3 in addition to PD-1 stain more intensely for cell surface phosphatidylserine and therefore appear more likely to perish than cells that are TIM-3⁺PD-1⁻. Senescent and dysfunctional characteristics of TIM-3⁺ Teffs that coexpress PD-1 have been well appreciated (13, 18, 19, 25). Signaling through PD-1 plays an important role in the exhaustion of Teffs (15, 31); however, PD-1 expression on T cells may not always be indicative of T cell dysfunction (32).

We tested the hypothesis that CD4⁺FoxP3⁺TIM-3⁺ Tregs, which are often PD-1⁺ like the CD4⁺FoxP3⁺TIM-3⁺ Teff population, are programmed for cell death and senescent, as detected by annexin V staining (a marker of early stage programmed cell death), or dead, as deduced by their failure to exclude vital dyes. In keeping with our prediction, 70% of CD4⁺FoxP3⁺TIM-3⁺ T cells were stained by annexin V; however, more than 95% were viable, as these cells exclude vital dyes. Thus, TIM-3 expression on Tregs unlike TIM-3⁺ Teffs may not serve as a marker of senescent Tregs. In fact, TIM-3⁺ Tregs, unlike TIM-3⁺ Teffs, proliferate vigorously. While, the blockade of inhibitory signals via PD-1 has been shown to rescue senescent Teffs (33), PD-1 blockade of CD4⁺FoxP3⁺TIM-3⁺ cells, which are already annexin V⁺, with anti-PD-1 in vitro (data not shown), did not influence the viability of TIM-3⁺ Tregs, as deduced by staining with annexin V and LIVE/DEAD blue vital dye. Subsequently, we analyzed the functional and molecular phenotypes of TIM-3⁺ Tregs. Unlike the dysfunctional status of TIM-3⁺ Teffs, TIM-3⁺ Tregs were better suppressors of Teff proliferation than TIM-3⁻ Tregs in an in vitro MLR. The increased frequency and expression of CTLA-4, CD39, IL-10, and TGF- β by TIM-3⁺ Tregs hints at the molecular basis for their increased potency in comparison to TIM-3⁻ Tregs. Paradoxical to the in vitro suppression assay, TIM-3⁺ Tregs, which are also annexin V⁺, demonstrated less

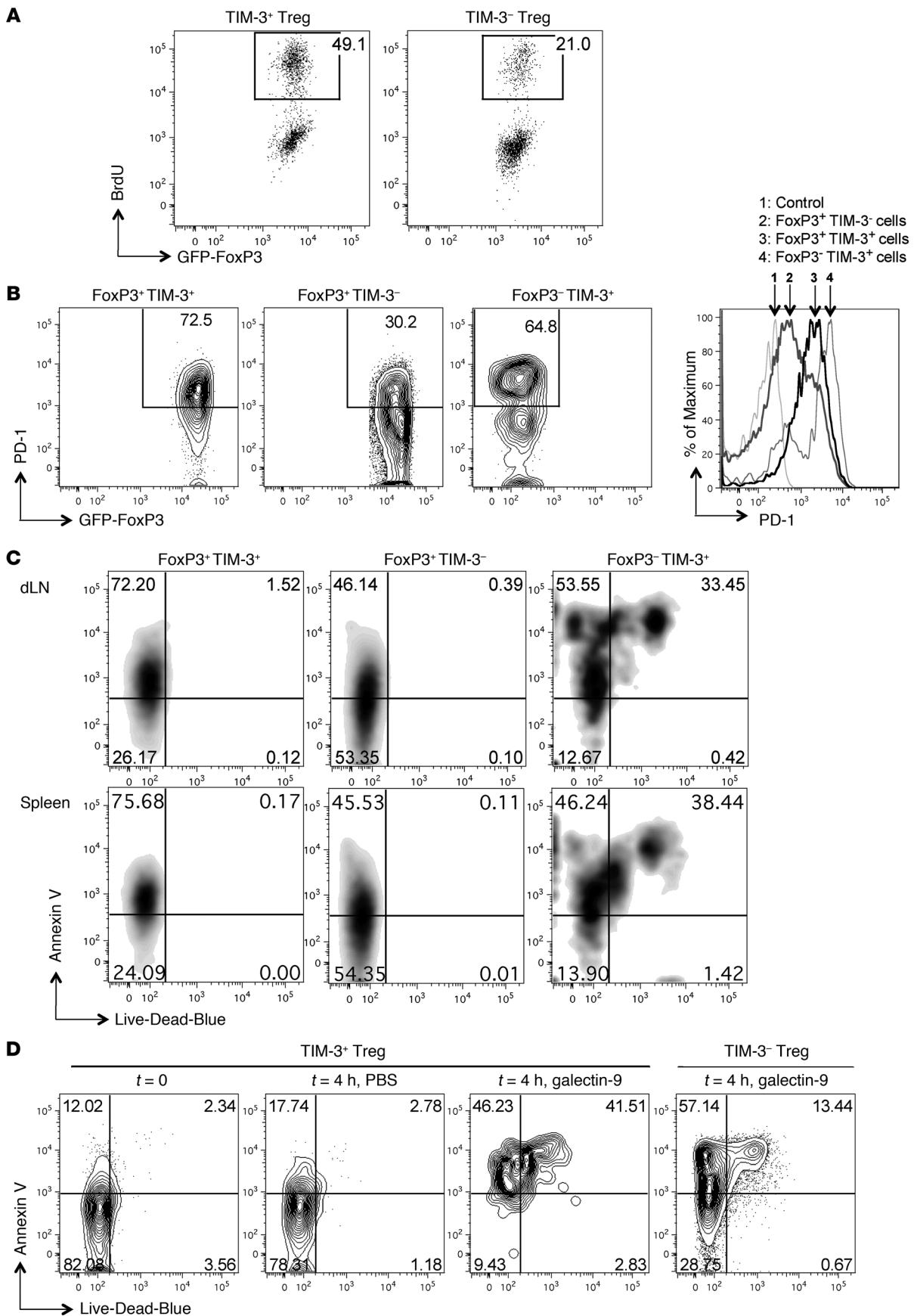




Figure 4

At the time of rejection of skin allografts, TIM-3⁺ Tregs in dLNs are proliferating, express surface PD-1, are programmed for cell death, and are galectin-9 sensitive. (A) Cells were analyzed from C57BL/6-KI recipients grafted with full-thickness body skin of BALB/c mice on day 7 after transplantation. Proliferation of TIM-3⁺ Tregs was compared with that of TIM-3⁻ Tregs in dLNs on day 7, as deduced via staining for BrdU (injected i.p. 24 and 12 hours prior to harvesting of cells). Representative plots of $n = 4$ animals are depicted. (B) The proportion of PD-1-expressing TIM-3⁺ Tregs in comparison with that of TIM-3⁻ Tregs and TIM-3⁺ Teffs in dLNs. In the histogram, 1 represents fluorescence minus one for PD-1 staining; 2 represents FoxP3⁺TIM-3⁻ cells; 3 represents FoxP3⁺TIM-3⁺ cells; and 4 represents FoxP3⁻TIM-3⁺ cells. Data are representative of $n = 5$ animals. (C) TIM-3⁺ Tregs were analyzed in comparison with TIM-3⁻ Tregs and TIM-3⁺ Teffs from dLNs for their ability to stain cell surface phosphatidyl serine with annexin V and exclude the LIVE/DEAD blue viability dye. Representative plots of $n \geq 8$ animals are shown. (D) Susceptibility of TIM-3⁺ Tregs to galectin-9-induced cell death was tested on GFP⁺FoxP3⁺ cells obtained by sorting from spleens of mice grafted with allogeneic skin on day 7. Cells were cultured with 0.5 μ M galectin-9/PBS for 4 hours ex vivo. TIM-3⁺ Tregs were assessed for staining with annexin V and LDB by flow cytometric analysis. Numbers represent the percentage of TIM-3⁺ or TIM-3⁻ Tregs or TIM-3⁺FoxP3⁻ cells as indicated in each panel. Data are representative of $n = 3$ experiments.

pronounced suppressive effects in an in vivo suppressive assay. The in vivo results do not invalidate the in vitro data, as the in vitro suppression assessment is made by culturing the cells with Teffs immediately, which may not affect the cell potency, and the assay lasts for 4 days. During the in vivo experiment, for over 15 days, the properties, including the viability and potency of this subpopulation, may have changed. It seems likely that many of the TIM-3⁺annexin V⁺ cells die. Moreover, cell surface phosphatidylserine⁺, TIM-3⁺ Tregs could not be rescued, even in the absence of ligands that trigger cell death, galectin-9, and PDL-1 (data not shown), indicating that these cells are indeed programmed to undergo cell death.

The presence of death molecules TIM-3 and PD-1 on this highly potent Treg subset may serve as a checkpoint, leading to the elimination of the TIM-3⁺ Treg subset after graft rejection. We asked what may account for the contraction of the TIM-3⁺ Treg subset after rejection. One factor must be disappearance of donor antigen after rejection. The sensitivity of TIM-3⁺ Treg to galectin-9 expressed on other graft-infiltrating mononuclear leukocytes may lead to death and contraction of TIM-3⁺ Tregs. While expression of other Treg effector molecules was increased on the TIM-3⁺ Treg subset, conspicuously the expression of galectin-9 was reduced drastically. We suspect that survival of the TIM-3⁺galectin^{hi} Treg subset is infrequent, because the expression of both the death molecules, TIM-3 and PD-1, and their ligands, galectin-9 and PD-L1, likely commit these cells to suicide.

In addition, this highly potent TIM-3⁺PD-1⁺galectin-9^{lo} Treg subset arises and expands in a microenvironment, as a result of continued T cell activation. Absence of antigen renders these annexin V⁺TIM-3⁺ and PD-1⁺ cells vulnerable to death, as they are programmed for apoptosis and are sensitive to galectin-9. The antigen-dependent disappearance of such a potent subset of immune-regulatory cells is suggestive of a homeostatic mechanism to deplete a highly potent Treg population that could otherwise hinder Teff immunity in the graft and dLNs.

Several biological effects have been attributed to the galectin-9/TIM-3 interaction (17, 34–36); however, in addition to galectin-9, TIM-3 binds to at least one other unidentified ligand (37). The

loss of TIM-3⁺ cells is attributed to galectin-9-induced apoptosis, based on in vitro studies (13), but a direct in vivo role has yet to be demonstrated directly. Our in vitro results are consistent with these findings, demonstrating that galectin-9 induces the loss of TIM-3⁺ Tregs. Su et al. recently demonstrated a dose-dependent, TIM-3-independent role for galectin-9 in the induction of apoptosis and cytokines in T cells. Wild-type and TIM-3KO Th1 cells were equally susceptible to galectin-9-induced apoptosis (38). Conclusions regarding the biological effects of the galectin-9/TIM-3 axis have been drawn based on galectin-9 administration (39, 40); in such a situation it is difficult to distinguish between the TIM-3-dependent and -independent effects of galectin-9. TIM-3 is classically believed to be a death molecule, due to its binding to galectin-9; however, a ligand-independent role of TIM-3 has been demonstrated to enhance cytokine production and proliferation by primary T cells after stimulation through CD3 and CD28 (41). TIM-3⁺ Tregs arising during the anti-allograft response are highly proliferative and have enhanced cytokine production, a function that seems to be independent of galectin-9.

Studying the ligand-receptor role of TIM-3⁺ Tregs by blocking the TIM-3/galectin-9 and PD-1/PDL-1 axes in transplant models suggested a concomitant affect on the TIM-3⁺ Treg and TIM-3⁺ Teff compartments. To study the role of galectin-9 and PDL-1 on the function and phenotype of TIM-3⁺PD-1⁺ Tregs in vivo, a FoxP3⁺ Treg lineage-specific TIM-3 and PD-1 double knockout, and perhaps an alloreactive T cell receptor transgene, is necessary. Moreover, a deeper understanding of the role that ligand interactions play in modulating TIM-3⁺ Treg functions in transplantation also awaits the discovery of the second ligand of TIM-3.

Thus, in this study we describe a highly potent subset of Tregs arising in response to alloantigens and expressing death molecules TIM-3 and PD-1. Contrary to our hypothesis, Tregs expressing these death molecules were not functionally impaired as Tregs. Instead TIM-3⁺PD-1⁺galectin-9^{lo} Tregs vigorously proliferated and robustly expressed Treg functional molecules. As compared with TIM-3⁻ Tregs, the TIM-3⁺ Tregs manifested enhanced immunoregulatory effector properties, but following rejection, i.e., in the absence of donor antigen cells and perhaps owing to expression of the TIM-3 and PD-1 death molecules, the TIM-3⁺ Tregs did not persist. It is interesting that, as the allograft response progresses, Tregs become more potent and prominent and yet express death molecules. Noted in parallel with phosphatidylserine positivity, TIM-3 and PD-1 expression by Tregs may represent an activation-induced stage in differentiation, manifested by increased potency and a commitment death. In this way local immunoregulation by antigen-driven Tregs is likely heightened and then largely ablated, thereby allowing subsequent local immune reactions to take place without undo and potentially harmful restraint by Tregs. Thus, the activation-induced expression of TIM-3 and PD-1 is not likely crucial to their immunoregulatory effector properties. Instead, the expression of these molecules manifests after several waves of proliferation and is expressed parallel with cell surface phosphatidylserine, possibly reflecting a means by which proliferating, graft-infiltrating antigen-reactive Tregs are cleared from the environment. Thus, the surge of Tregs with increased potency after multiple waves of proliferation is balanced by ensuring their clearance. The apparent result of these events is to produce both potent and short-lived Tregs that are cleared from the microenvironment after rejection. Hence, the immune response to microbes within this microenvironment is not permanently hampered.

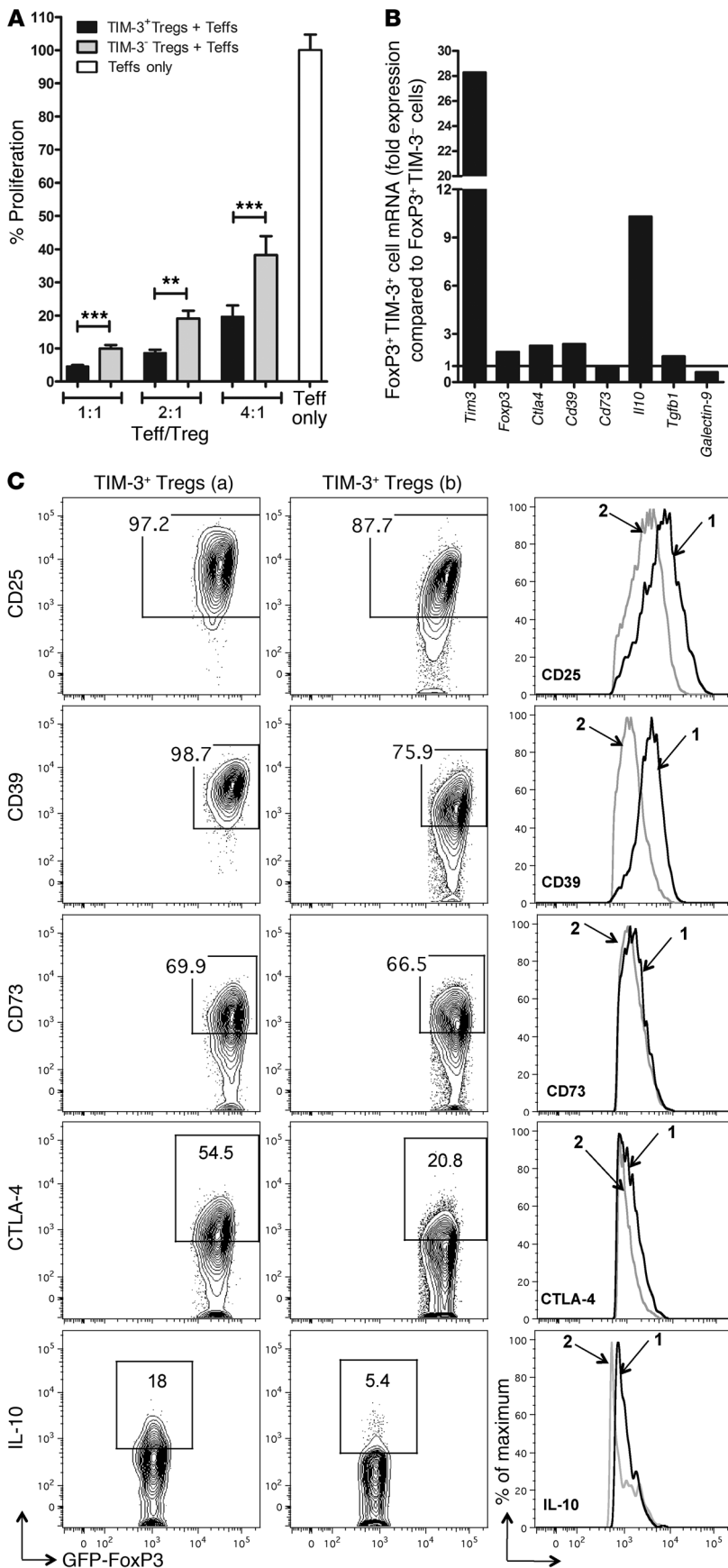
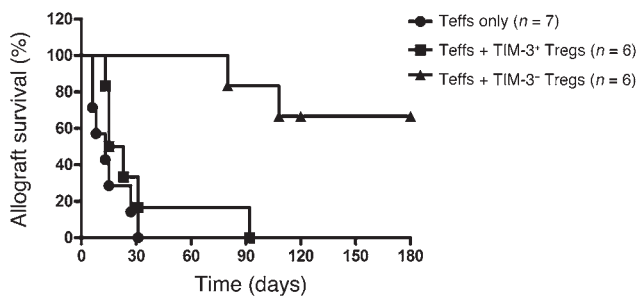


Figure 5

CD4⁺TIM-3⁺ Tregs are potent suppressors of Teff proliferation in an in vitro MLR culture and robustly express Treg markers. **(A)** In an MLR culture, naive CD4⁺GFP⁻ Teffs from spleens of BALB/c-KI mice were stimulated with irradiated CD90⁻ splenocytes from BALB/c-KI mice for 3 days in the presence or absence of Tregs. Sorted CD4⁺GFP⁺TIM-3⁺/TIM-3⁻ Tregs were obtained from spleens of BALB/c-KI mice injected with DBA/2 DST 5 days prior to harvesting. T cell proliferation in these cultures was analyzed by the mean values of incorporated thymidine of duplicate/triplicate wells and compared with that of MLR cultures with Teff alone (normalized as 100%). Data are represented as mean ± SEM; n = 3 independent experiments done in duplicate, triplicates, or quadruplicates leading to a total of ≥ 8 independent values for each condition. **P = 0.002; ***P < 0.001. **(B)** TIM-3⁺GFP⁺FoxP3⁺ and TIM-3⁻GFP⁺FoxP3⁺ cells were sorted from harvested dLNs of 30 to 35 C57BL/6-KI mice grafted with BALB/c skin on day 7. RNA was isolated from sorted TIM-3⁺GFP⁺FoxP3⁺ and TIM-3⁻GFP⁺FoxP3⁺ populations. Gene expression of various markers was assessed by quantitative real-time PCR. Data are representative of 3 independent experiments. **(C)** CD4⁺TIM-3⁺ Tregs and CD4⁺TIM-3⁻ Tregs harvested from the dLNs on day 7 were stained and analyzed by flow cytometry for various Treg functional markers as shown. Arrows in the histograms depict TIM-3⁻ Tregs (a) and TIM-3⁺ Tregs (b). Numbers represent the percentage of TIM-3⁺ and TIM-3⁻ Tregs, respectively. n ≥ 5 mice.

**Figure 6**

Adoptively transferred TIM-3⁺ Tregs prolong graft survival less profoundly in an in vivo suppression assay compared with TIM-3⁻ Tregs. BALB/c-KI-TIM-3⁺/TIM-3⁻ Tregs were sorted from spleens of DBA/2 DST-injected BALB/c mice. Teffs with or without TIM-3⁺/TIM-3⁻ Tregs (Teff/Treg, 2:1) were adoptively transferred into DBA/2-grafted BALB/c-*Rag2*^{-/-} mice, and graft survival was recorded. The survival of grafted skin was prolonged in both Treg- and Teff-injected groups, albeit graft survival was more prolonged by TIM-3⁻ Tregs in comparison to TIM-3⁺ Tregs. *n* = 2 independent experiments, total of ≥ 6 mice per group.

Methods

Mice. C57BL/6 (H-2b), BALB/c (H-2d), and DBA/2 (H-2d) mice were purchased from The Jackson Laboratory, and BALB/c *Rag2*^{-/-} mice were purchased from Taconic Farms Inc. The C57BL/6 Foxp3-GFP knockin (C57BL/6-KI) and BALB/c Foxp3-GFP knockin (BALB/c-KI) mice have been previously described (42). All animals were housed under standard conditions, and the studies were approved by the Animal Institutional Review Board at Beth Israel Deaconess Medical Center.

Antibodies. Anti-CD4 was purchased from BioLegend; anti-CD3, anti-CD28, anti-Vβ6, and anti-Vβ8 TCR were purchased from BD Pharmingen; and all other monoclonal antibodies were purchased from eBioscience. Anti-TIM-3 antibody clones RMT-3-23 and 8B.2C.12 were used to stain TIM-3 in C57BL/6 and BALB/c mouse cells, respectively.

Cell preparation. CD4⁺ T cells were enriched from monodispersed splenic mononuclear leukocytes by negative selection using the Easy-Sep Mouse CD4⁺ T Cell Enrichment Kit (Stem Cell Technologies). CD4⁺ subpopulations, namely CD4⁺GFP(Foxp3)⁺, CD4⁺GFP(Foxp3)⁻, CD4⁺GFP(Foxp3)⁺TIM-3⁺, and CD4⁺GFP(Foxp3)⁺TIM-3⁻ cells, were obtained by cell sorting (BD FACSAria cell sorter, BD Biosciences).

Skin transplantation. Full-thickness skin grafts of 1 to 2 cm in diameter were obtained from the flanks of donor mice and transplanted onto the lateral thorax of recipients (43). Graft rejection was defined as the first day on which the entire graft was necrotic (43).

Cell staining and flow cytometry. Donor strain monodispersed spleen and LN mononuclear leukocytes were suspended in FACS buffer (PBS [Cellgro] with 1% FBS [Gemini Bio-Products]). To block Fc receptor-mediated binding of antibodies, mononuclear leukocytes were suspended in FACS buffer with 5% mouse serum (Sigma-Aldrich) for 20 minutes. These cells were washed, placed on ice for 30 minutes, and stained with fluorochrome-conjugated antibodies. Cells were washed twice in buffer and isolated using the LSR II flow-cytometer (BD Biosciences). Data analysis for these experiments was performed using FlowJo software (Tree Star). All cells obtained by collagenase digestion of the allograft were also analyzed by flow cytometry. CD4⁺GFP⁺ cells constitute a small number of cells obtained from the graft, and, hence, TIM-3⁺ Treg count was also low, accounting for the low-quality histogram. In some studies, 2 mg BrdU (BD Pharmingen) was injected i.p. 24 and 12 hours prior to harvesting tissue, and intracellular BrdU staining was analyzed as specified by the manufacturer. In the flow cytometric experiments, total cell counts were determined using Absolute Counting Tubes BD TruCount (BD Biosciences) as specified by the manufacturer. Intracellular staining for IL-10 was performed on LN cells after activation with Leukocyte Activation Cocktail (BD Biosciences) and following cell permeabilization and fixation with the BD Cytofix/Cytoperm Fixation/Permeabilization Solution Kit (BD Biosciences) using the manufacturer's protocol.

DST. On day 0, BALB/c-KI mice received DST i.v. with 10⁷ DBA/2 or BALB/c splenic cells. On day 5 after transfusion, recipient spleen cells

were analyzed by flow cytometry for expression of GFP(Foxp3), TIM-3, and Vβ6 or Vβ8 TCR molecules. For studies in lymphopenic mice, splenic CD4⁺GFP(Foxp3)⁺TIM-3⁻ cells were sorted from BALB/c-KI mice 5 days after DBA/2 DST. CD4⁺GFP(Foxp3)⁺TIM-3⁻ cells (0.5 × 10⁶ cells per mouse) were injected i.v. into BALB/c *Rag2*^{-/-} mice, which had been previously grafted with full-thickness DBA/2 body skin. Three weeks later recipient, spleen cells were analyzed by flow cytometry.

Real-time quantitative PCR. Total cellular RNA was extracted using RNeasy Mini and Micro Kits (Qiagen) and reverse transcribed into cDNA by the ABI PRISM TaqMan reverse transcription method. Expression for genes of interest was analyzed in CD4⁺GFP(Foxp3)⁺TIM-3⁺, CD4⁺GFP(Foxp3)⁺TIM-3⁻, and CD4⁺GFP(Foxp3)⁻TIM-3⁺ cell populations on day 7 after transplantation by cell sorting from graft dLNs of C57BL/6 Foxp3-GFP-KI mice grafted with BALB/c skin. Primer sequences were obtained from the Harvard Medical School Primer Bank database (<http://pga.mgh.harvard.edu/primerbank/>) and then purchased from Integrated DNA Technologies Inc. Quantitative real-time PCR was performed via ABI PRISM 7900HT Sequence Detection System (Applied Biosystems). Transcript levels were calculated according to the 2^{-ΔΔCt} method, normalized to the expression of GAPDH, as described by the manufacturer, and expressed in arbitrary units.

Induction and expansion of TIM-3⁺Foxp3⁺ Tregs in vitro. Sorted splenic CD4⁺GFP(Foxp3)⁺, CD4⁺GFP(Foxp3)⁺TIM-3⁺, or CD4⁺GFP(Foxp3)⁺TIM-3⁻ cells from untreated C57BL/6 mice were cultured in complete media (RPMI 1640 medium supplemented with 10% FBS, 100 U/ml penicillin/streptomycin, 2 mM glutamine, 1 mM MEM-sodium pyruvate, 0.1 mM nonessential amino acids, and 50 μM 2-β mercaptoethanol) with soluble anti-CD28 mAb (1 μg/ml) in the presence or absence of plate-bound anti-CD3 mAb (10 μg/ml) and IL-2 (10 ng/ml) (eBiosciences or PeproTech Inc.) for 4 days. Induction of TIM-3⁺Foxp3⁺ expression was determined by flow cytometry by gating on the CD4⁺GFP(Foxp3)⁺ cells and presented as the percentage of total CD4⁺Foxp3⁺ cells. CD4⁺GFP(Foxp3)⁺TIM-3⁺ cells were interacted with anti-PD-1 antibody, annexin V (eBioscience), and LIVE/DEAD-blue (LDB) (Invitrogen) as per the manufacturer's instructions and then analyzed by flow cytometry.

Cell death analysis after interaction with galectin-9. Purified splenic CD4⁺GFP(Foxp3)⁺ cells were obtained by sorting on day 7 after transplantation from C57BL/6-KI mice grafted with BALB/c skin. Cells were plated for 4 hours at a density of 2 × 10⁵ cells per well in the presence of PBS or 0.5 μM galectin-9 (gift from GalPharma Co. Ltd.) as described previously (13). The impact of galectin-9 interaction on survival of CD4⁺GFP(Foxp3)⁺ TIM-3⁺ and CD4⁺GFP(Foxp3)⁺ TIM-3⁻ cells was evaluated by staining with annexin V and LDB using manufacturer's instructions.

MLR-based cell suppression assay and in vivo suppression study. Stimulator cells (1 × 10⁵ cells per well) were obtained from BALB/c splenic mononuclear leukocytes by depletion of T cells using the EasySep



Mouse CD90 Positive Selection Kit (Stem Cell Technologies), gamma-irradiated with 30 Gy, and placed into round-bottomed 96-well plates. The naive CD4⁺GFP(Foxp3)⁻ Tregs were sorted from BALB/c-KI mice. Treg CD4⁺GFP(Foxp3)⁺TIM-3⁻ or CD4⁺GFP(Foxp3)⁺TIM-3⁺ cells were obtained by sorting from spleens of the BALB/c-KI mice that had been transfused 5 days prior with DBA/2 spleen cells. Varying ratios of Treg/Tregs were plated in duplicates or triplicates. Complete media was supplemented with anti-CD3 (10 µg/ml). Cells were incubated at 37°C for 72 hours and were pulsed with [³H]TdR (1 µCi/well; Perkin Elmer) during the last 16 hours of culture cells. Incorporation of [³H]TdR was analyzed by a microbeta scintillation counter (Wallac Trilux, Perkin Elmer). For in vivo suppression assay, similarly obtained Tregs and Tregs were adoptively transferred at a ratio of 2:1 into BALB/c-Rag2^{-/-} mice that were grafted with DBA/2 skin 10 days prior.

Statistics. Data were analyzed using Prism5 (GraphPad Software Inc.), and the results were expressed as mean ± SEM. In the analysis, comparisons were made using the Student's *t* test, and *P* < 0.05 was considered significant.

Acknowledgments

We thank Vasilis Toxavidis and John Tigges at the BIDMC flow cytometry core facility for their expertise in cell sorting. This work was supported by JDRF grant 1-2007-551 (to W. Gao); NIH grants P01 AI073748, P01 NS038037, and R01 NS045937 (to V.K. Kuchroo); NIH grants AI37691 and AI41521 (to L.A. Turka); and NIH grants P0AIGF41521 and P01 AI073748 (to T.B. Strom). S. Gupta was supported by NIH grant P01 AI073748-02, and T.B. Thornley was supported by NIH grant P01 AI041521-12S1.

Received for publication September 16, 2010, and accepted in revised form March 29, 2012.

Address correspondence to: Terry B. Strom, The Transplant Institute, Beth Israel Deaconess Medical Center, 330 Brookline Avenue – E/CLS 608, Boston, Massachusetts 02215, USA. Phone: 617.735.2880; Fax: 617.735.2902; E-mail: tstrom@bidmc.harvard.edu.

1. Miossec P, Korn T, Kuchroo VK. Interleukin-17 and type 17 helper T cells. *N Engl J Med.* 2009;361(9):888–898.
2. Strom TB, et al. The Th1/Th2 paradigm and the allograft response. *Curr Opin Immunol.* 1996;8(5):688–693.
3. Kang SM, Tang Q, Bluestone JA. CD4⁺CD25⁺ regulatory T cells in transplantation: progress, challenges and prospects. *Am J Transplant.* 2007;7(6):1457–1463.
4. Wing K, Sakaguchi S. Regulatory T cells exert checks and balances on self tolerance and autoimmunity. *Nat Immunol.* 2010;11(1):7–13.
5. Kuchroo VK, Meyers JH, Umetsu DT, DeKruyff RH. TIM family of genes in immunity and tolerance. *Adv Immunol.* 2006;91:227–249.
6. Mariat C, Sanchez-Fueyo A, Alexopoulos SP, Kenny J, Strom TB, Zheng XX. Regulation of T cell dependent immune responses by TIM family members. *Philos Trans R Soc Lond B Biol Sci.* 2005;360(1461):1681–1685.
7. Sanchez-Fueyo A, et al. Tim-3 inhibits T helper type 1-mediated auto- and alloimmune responses and promotes immunological tolerance. *Nat Immunol.* 2003;4(11):1093–1101.
8. Kuchroo VK, Dardalhon V, Xiao S, Anderson AC. New roles for TIM family members in immune regulation. *Nat Rev Immunol.* 2008;8(8):577–580.
9. Monney L, et al. Th1-specific cell surface protein Tim-3 regulates macrophage activation and severity of an autoimmune disease. *Nature.* 2002;415(6871):536–541.
10. Hastings WD, et al. TIM-3 is expressed on activated human CD4⁺ T cells and regulates Th1 and Th17 cytokines. *Eur J Immunol.* 2009;39(9):2492–2501.
11. Anderson AC, et al. Promotion of tissue inflammation by the immune receptor Tim-3 expressed on innate immune cells. *Science.* 2007; 318(5853):1141–1143.
12. Anderson AC, Anderson DE. TIM-3 in autoimmunity. *Curr Opin Immunol.* 2006;18(6):665–669.
13. Zhu C, et al. The Tim-3 ligand galectin-9 negatively regulates T helper type 1 immunity. *Nat Immunol.* 2005;6(12):1245–1252.
14. Sabatos CA, et al. Interaction of Tim-3 and Tim-3 ligand regulates T helper type 1 responses and induction of peripheral tolerance. *Nat Immunol.* 2003;4(11):1102–1110.
15. Day CL, et al. PD-1 expression on HIV-specific T cells is associated with T-cell exhaustion and disease progression. *Nature.* 2006;443(7109):350–354.
16. Jin HT, et al. Cooperation of Tim-3 and PD-1 in CD8 T-cell exhaustion during chronic viral infection. *Proc Natl Acad Sci U S A.* 2010;107(33):14733–14738.
17. Zhou Q, et al. Coexpression of Tim-3 and PD-1 identifies a CD8⁺ T-cell exhaustion phenotype in mice with disseminated acute myelogenous leukemia. *Blood.* 2011;117(17):4501–4510.
18. Jones RB, et al. Tim-3 expression defines a novel population of dysfunctional T cells with highly elevated frequencies in progressive HIV-1 infection. *J Exp Med.* 2008;205(12):2763–2779.
19. Koguchi K, Anderson DE, Yang L, O'Connor KC, Kuchroo VK, Hafler DA. Dysregulated T cell expression of TIM3 in multiple sclerosis. *J Exp Med.* 2006;203(6):1413–1418.
20. Sakaguchi S, et al. Foxp3⁺ CD25⁺ CD4⁺ natural regulatory T cells in dominant self-tolerance and autoimmune disease. *Immunol Rev.* 2006;212:8–27.
21. Wood KJ, Sakaguchi S. Regulatory T cells in transplantation tolerance. *Nat Rev Immunol.* 2003;3(3):199–210.
22. Gao W, et al. Treg versus Th17 lymphocyte lineages are cross-regulated by LIF versus IL-6. *Cell Cycle.* 2009;8(9):1444–1450.
23. MacDonald HR, Pedrazzini T, Schneider R, Louis JA, Zinkernagel RM, Hengartner H. Intrathymic elimination of Mlsa-reactive (V beta 6⁺) cells during neonatal tolerance induction to Mlsa-encoded antigens. *J Exp Med.* 1988;167(6):2005–2010.
24. Raimondi G, Shufesky WJ, Tokita D, Morelli AE, Thomson AW. Regulated compartmentalization of programmed cell death-1 discriminates CD4⁺CD25⁺ resting regulatory T cells from activated T cells. *J Immunol.* 2006;176(5):2808–2816.
25. Golden-Mason L, et al. Negative immune regulator Tim-3 is overexpressed on T cells in hepatitis C virus infection and its blockade rescues dysfunctional CD4⁺ and CD8⁺ T cells. *J Virol.* 2009;83(18):9122–9130.
26. Salomon B, et al. B7/CD28 costimulation is essential for the homeostasis of the CD4⁺CD25⁺ immunoregulatory T cells that control autoimmune diabetes. *Immunity.* 2000;12(4):431–440.
27. Deaglio S, et al. Adenosine generation catalyzed by CD39 and CD73 expressed on regulatory T cells mediates immune suppression. *J Exp Med.* 2007;204(6):1257–1265.
28. Asseman C, Mauze S, Leach MW, Coffman RL, Powrie F. An essential role for interleukin 10 in the function of regulatory T cells that inhibit intestinal inflammation. *J Exp Med.* 1999;190(7):995–1004.
29. Chen ML, et al. Regulatory T cells suppress tumor-specific CD8 T cell cytotoxicity through TGF-beta signals in vivo. *Proc Natl Acad Sci U S A.* 2005;102(2):419–424.
30. Sakaguchi S, Sakaguchi N, Asano M, Itoh M, Toda M. Immunologic self-tolerance maintained by activated T cells expressing IL-2 receptor alpha-chains (CD25). Breakdown of a single mechanism of self-tolerance causes various autoimmune diseases. *J Immunol.* 1995;155(3):1151–1164.
31. Trautmann L, et al. Upregulation of PD-1 expression on HIV-specific CD8⁺ T cells leads to reversible immune dysfunction. *Nat Med.* 2006; 12(10):1198–1202.
32. Sadagopal S, et al. Enhanced PD-1 expression by T cells in cerebrospinal fluid does not reflect functional exhaustion during chronic human immunodeficiency virus type 1 infection. *J Virol.* 2010;84(1):131–140.
33. Freeman GJ, Wherry EJ, Ahmed R, Sharpe AH. Reinvigorating exhausted HIV-specific T cells via PD-1-PD-1 ligand blockade. *J Exp Med.* 2006;203(10):2223–2227.
34. Bi S, Hong PW, Lee B, Baum LG. Galectin-9 binding to cell surface protein disulfide isomerase regulates the redox environment to enhance T-cell migration and HIV entry. *Proc Natl Acad Sci U S A.* 2011;108(26):10650–10655.
35. Nakayama M, et al. Tim-3 mediates phagocytosis of apoptotic cells and cross-presentation. *Blood.* 2009;113(16):3821–3830.
36. Sehrawat S, Suryawanshi A, Hirashima M, Rouse BT. Role of Tim-3/galectin-9 inhibitory interaction in viral-induced immunopathology: shifting the balance toward regulators. *J Immunol.* 2009;182(5):3191–3201.
37. Cao E, et al. T cell immunoglobulin mucin-3 crystal structure reveals a galectin-9-independent ligand-binding surface. *Immunity.* 2007;26(3):311–321.
38. Su EW, Bi S, Kane LP. Galectin-9 regulates T helper cell function independently of Tim-3. *Glycobiology.* 2010;21(10):1258–1265.
39. Nagahara K, et al. Galectin-9 increases Tim-3⁺ dendritic cells and CD8⁺ T cells and enhances antitumor immunity via galectin-9–Tim-3 interactions. *J Immunol.* 2008;181(11):7660–7669.
40. Sakai K, et al. Galectin-9 ameliorates acute GVH disease through the induction of T-cell apoptosis. *Eur J Immunol.* 2011;41(1):67–75.
41. Lee J, et al. Phosphotyrosine-dependent coupling of Tim-3 to T-cell receptor signaling pathways. *Mol Cell Biol.* 2011;31(19):3963–3974.
42. Bettelli E, et al. Reciprocal developmental pathways for the generation of pathogenic effector TH17 and regulatory T cells. *Nature.* 2006;441(7090):235–238.
43. Markees TG, et al. Long-term survival of skin allografts induced by donor splenocytes and anti-CD154 antibody in thymectomized mice requires CD4⁺ T cells, interferon-gamma, and CTLA4. *J Clin Invest.* 1998;101(11):2446–2455.